Impact of Fabrication Non-Uniformity on Chip-Scale Silicon Photonic Integrated Circuits

L. Chrostowski, X. Wang, J. Flueckiger, Y. Wu, Y. Wang, S. Talebi Fard

Department of Electrical and Computer Engineering, University of British Columbia, V6R 1T3, Canada

Abstract: This study of 371 identical resonators on a 16x9 mm chip fabricated by a silicon photonics foundry reveals a strong linear correlation between the physical distance between devices and the variability in their wavelength mismatch.

1. Introduction

Photonic integrated circuits (PICs) often require precise matching of the central wavelength and the waveguide propagation constants between components on a chip (e.g., ring modulators, optical filters), particularly for wavelength division multiplexing. Understanding the fabrication variability is critical to developing strategies (e.g., thermal tuning) for system implementation, and for determining the cost implications for such compensation strategies (e.g., power consumption). Previous work on fabrication non-uniformity including intra-device uniformity (e.g., CROWs [1]), within wafer, wafer-to-wafer, and batch-to-batch variations identified silicon thickness variation as the primary concern [2–5]. This work focuses on variation between devices within a chip, to gain an understanding of the variations as a function of the distance typically seen in PICs, namely ranging from hundreds of microns to millimetres. The implication is the importance of very compact layouts when components need to be matched, leading to reduced (but not eliminated) trimming cost.

2. Design and Measurement

This study involves the fabrication, test, and analysis of 371 identical racetrack resonators on a 16x9 mm chip fabricated by IME's silicon photonics foundry. The measured die was located close to the centre of the wafer. The unit cell for testing is shown in Fig 1a, and consists of two fibre grating couplers (FGCs) designed for 1550 nm quasi-TE operation [6], 220 nm thick silicon on insulator (SOI) strip waveguides with a 500 nm width, connected to a TE polarization racetrack resonator with a 12 μm radius, and a directional coupler with a 4.5 μm length and 200 nm gap. Devices were placed between 60 μm and 18 mm apart. To obtain insight into the statistics of the wavelength variation, the 371 resonators were compared with each other resonator on the chip, for a total of (371 choose 2) = 68635 combinations; a histogram of these distances is shown inset in Fig 1a.

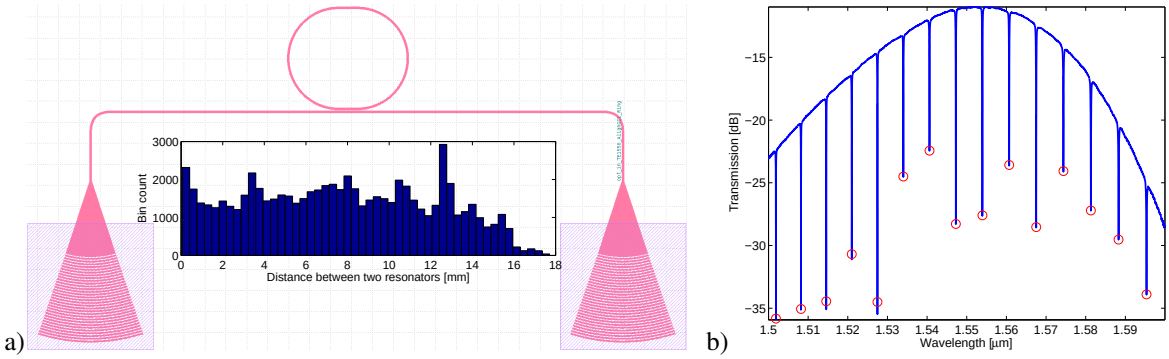

Fig. 1. **a)** Mask layout of the racetrack resonator with a pair of fibre grating couplers on a 127 μm pitch for automated optical testing; inset: histogram for the distribution of the distances between devices, for the 68635 combinations. Note that $>$ 1300 comparison were made for resonators less than 200 μm apart. **b)** Optical spectrum of a typical device with resonance wavelengths identified.

Automated measurements were performed on all devices. The spectra were sampled at a 10 pm resolution for rapid sweeping; the extinction ratios were thus limited due to under-sampling. Typical Q factors were 10-30k. Fibre-fibre insertion loss was typically 11 dB. A peak finding algorithm was used for data analysis. A typical spectrum is shown in Fig 1b, with a free-spectral range (FSR) of ~7 nm.

3. Results and Discussion

It was found that the wavelength variability across the chip was greater than the FSR of the device. Hence it was not possible to directly determine the variation of the resonance wavelength since it was not known which mode was which from the spectrum by inspection. The following method was applied: 1) From the peak position information, and knowing the resonator length, the group index (n_g) of the ring waveguide was calculated by $FSR = c/n_g L$. 2) The n_g and wavelength for all resonators and all peaks was plotted, Fig 2a. A clear relationship is evident, where each downward diagonal line corresponds to a resonator azimuthal mode, m. This relationship originates from **a)** the resonator wavelength being dependant on the effective index of the waveguide via $m\lambda_m = n_{\text{eff}}(\lambda_m)L$, and **b)** the physical variations (e.g., thickness, width) that change the effective index of the waveguide, n_{eff}, simultaneously affect the group index. 3) Using this correlation, it is possible to select all the data points that belong to one mode by finding the points closest to a chosen line, as drawn in Fig 2a. It is seen that the maximum variation of the resonator wavelength across the chip is slightly greater than 10 nm. Fig 2b shows a map of the resonator wavelength versus position.

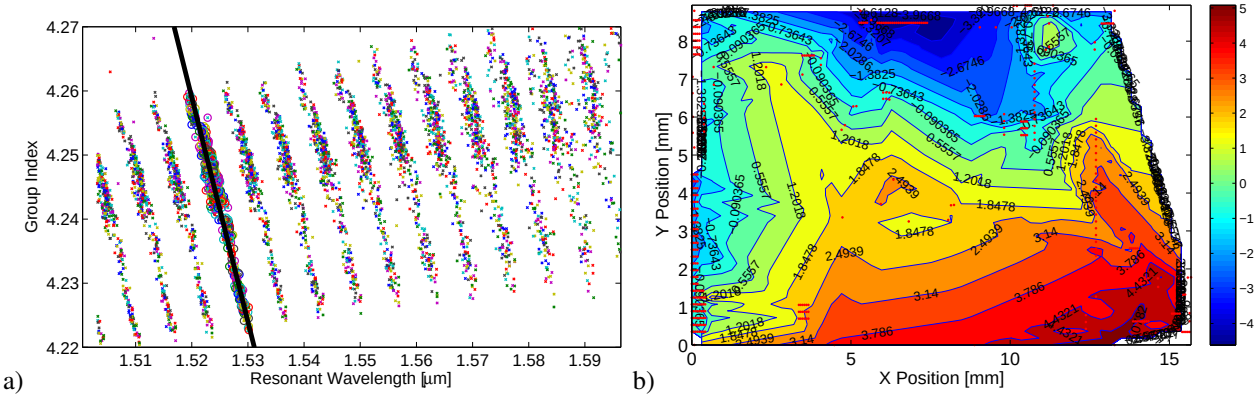

Fig. 2. **a)** Extracted group index versus resonance wavelength for all resonators. **b)** Resonance wavelength deviation contours (in nm) versus physical position on the chip. Resonance is chosen from the mode selected from the line in Fig 2a. The "0" contour corresponds to the mean wavelength.

Next, we compare each pair of resonators, and calculate the difference in resonator wavelength (y axis), versus the distance between each pair of devices (x axis), as shown in the scatter plot in Fig 3a. This clearly shows that the worst-case deviation between two resonators is approximately linearly proportional to the distance between them; for example two resonators that are 1 mm apart show at most a 4 nm difference in wavelength, however when they are 4 mm apart, the difference increases to 8 mm. These points were statistically analyzed, and represented using box plots in Fig 3a. This was done by binning the points in distance (1 mm bins for the first few mm, larger for longer distances). The probability distribution functions for the wavelength mismatch are shown inset in Fig 3a. Curiously the distributions become nearly uniform with a sharp maximum cut-off for large enough distance ranges (e.g., 5-6 mm). For distances $\geq$ 5 mm, the variations show trends of "bunching", which is likely due to the arrangement of the resonators on the layout and the limited sample size.

Important information from this analysis includes the median, which increases linearly up to a distance of 5 mm. This indicates that the fabrication variations are correlated over short distance scales. At short distances, a line of best fit for the median wavelength deviation versus distance is $\bar{\lambda}_{\text{ring}} = 0.47nm/mm \cdot d + 0.35nm$, as shown in Fig. 3b. This gives the expected value for the deviation between two resonant devices on a chip as a function of distance. The y-intercept also predicts that two resonators at a distance 0 apart would have a variability of 0.35 nm. Assuming a heater efficiency of 0.8 mW/FSR [7], this suggests that we will need on average $0.35nm/7nmFSR \cdot 0.8mW/FSR = 0.04mW$ per pair of resonators that need matching, for example in a two-ring Vernier filter [8].

Using the same methodology, an analysis was done on the grating couplers' peak wavelength (which is $\lambda_{\text{FGC}} =$

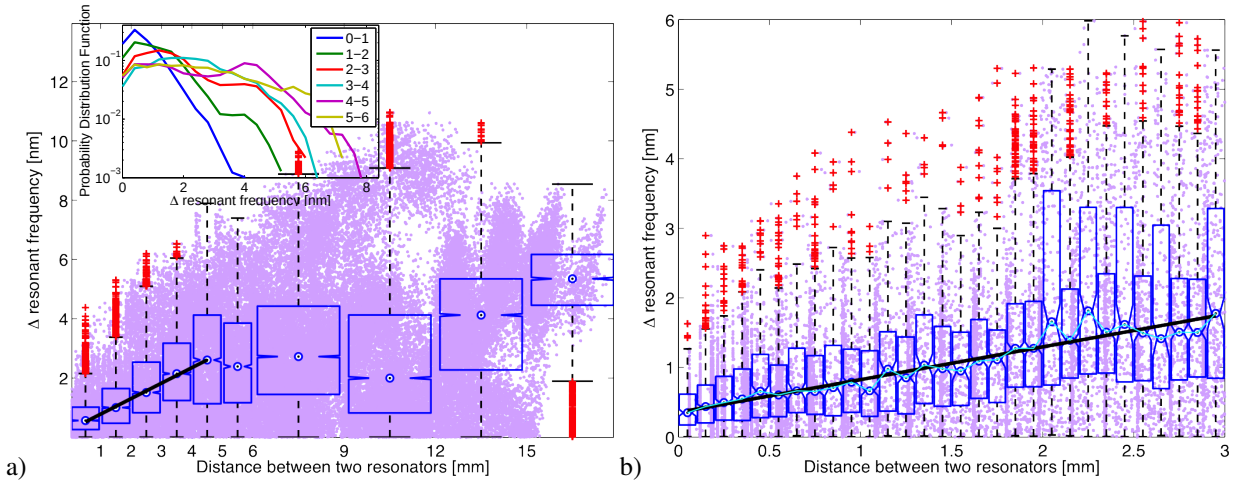

Fig. 3. **a)** Scatter plot of the difference in resonator wavelength, versus distance between them (68635 data points in purple). Overlaid boxplot for statistics with bins for distances ranging 0–1 mm, 1–2, 2–3, 4–5, 5–6, 6–9, 9–12, 12–15, and 15–18 mm. The box represents the central 50% of the data. The middle circles indicate the median. The two vertical lines extend maximally to 1.5 times the height of the box but not past the range of the data. Outliers are marked as red ("+") markers. Notches are the 95% confidence intervals. Inset: Probability distribution functions for the expected wavelength difference between resonators 0–1 mm apart, etc. **b)** Scatter and box plot of the difference in resonator wavelength, versus distance between them, for distances ranging from 0 to 3 mm, with boxes in 100 μm steps.

1.555μm in Fig 1b). The wavelength variation similarly increases linearly from 0 to 5 mm, with an expected average variation of $\bar{\lambda}_{\text{FGC}} = 1.33nm/mm \cdot d + 0.52nm$. However, variations across the chip for longer distances can reach as large as 30 nm. We note that the variations in resonator and grating coupler wavelengths have different spatial and statistical distributions, suggesting they have different physical origins. In addition to the SOI thickness, the grating couplers are primarily sensitive to etch depth. These grating couplers have their central wavelength with a sensitivity to SOI thickness of 1.82 nm/nm, to etch depth of 1.9 nm/nm, and to the width of the grating fingers of 0.215 nm/nm.

The results of this study may be useful for PIC system optimization, for example to calculate the power consumption required for trimming in large arrays of microring resonator or Mach-Zehnder switches. The parameters for the expected variability of resonators and grating couplers may also be useful for process monitoring and optimization, and for binning chips before packaging based on expected performance.

References

1. M. L. Cooper, *et al.*, "235-ring coupled-resonator optical waveguides," *Conf. Lasers and Electro-Optics*, 2010.
2. W. A. Zortman, *et al.*, "Silicon photonics manufacturing," *Opt. Express*, 18, pp. 23 598–23 607, 2010.
3. A. Krishnamoorthy, *et al.*, "Exploiting CMOS manufacturing to reduce tuning requirements for resonant optical devices," *IEEE Photonics Journal*, 3, pp. 567–579, 2011.
4. S. K. Selvaraja, *et al.*, "Subnanometer linewidth uniformity in silicon nanophotonic waveguide devices using CMOS fabrication technology," *IEEE J. Selected Topics in Quantum Electronics*, 16, pp. 316–324, 2010.
5. X. Wang, *et al.*, "Narrow-band waveguide Bragg gratings on SOI wafers with CMOS-compatible fabrication process," *Opt. Express*, 20, pp. 15 547–15 558, Jul 2012.
6. Y. Wang, *et al.*, "Universal grating coupler design," *Proc. SPIE*, 8915, p. 89150Y, 2013.
7. T.-Y. Liow, *et al.*, "Silicon optical interconnect device technologies for 40 Gb/s and beyond," *IEEE JSTQE*, 19, p. 8200312, 2013.
8. R. Boeck, *et al.*, "FSR-eliminated vernier racetrack resonators using grating-assisted couplers," *IEEE Photonics Journal*, 5, p. 2202511, 2013.

We acknowledge CMC Microsystems for access to fabrication at A*STAR IME; Mentor Graphics and Lumerical Solutions for design software; and NSERC for funding.